Analysis of Bridge−Mediated Pathways for Long−Range Charge Transfer Systems

ARTICLE *in* THE JOURNAL OF PHYSICAL CHEMISTRY B · SEPTEMBER 2006

Impact Factor: 3.3 · DOI: 10.1021/jp062941p · Source: PubMed

THE JOURNAL OF PHYSICAL CHEMISTRY B LETTERS

2006, *110,* 16803−16807
Published on Web 08/08/2006

Analysis of Bridge-Mediated Pathways for Long-Range Charge Transfer Systems

Eunji Sim* and Heeyoung Kim

Department of Chemistry, Yonsei University, 134 Sinchondong Seodaemungu, Seoul 120-749, Korea

Received: May 14, 2006; In Final Form: June 26, 2006

With the density matrix decomposition scheme of the path integral method, an accurate quantitative analysis on bridge-mediated pathways in long-range charge transfer processes is presented. Unlike a donor−bridge−acceptor triad, a long-range charge transfer process with a number of bridges has additional pathways in which charges always migrate through bridges but not necessarily by incoherent nearest-neighbor hopping. By employing the density matrix decomposition and sorting the incoherent nearest-neighbor and the coherent next-nearest-neighbor hopping pathways, respective contributions to the charge transfer are evaluated quantitatively. Numerical results of two series of configurations with varying degrees of coherence within the system have found that, depending on the configuration, the contribution of the coherent pathways other than superexchange pathways is significant. In the presence of the coherence, long-range charge transfer dynamics may be dominated by the through-bridge mechanism that consists of the coherent through-bridge pathways as well as the incoherent nearest-neighbor hopping pathways.

1. Introduction

Conventionally, two representative mechanisms have been considered for the long-range charge transfer (CT) processes: incoherent hopping and coherent superexchange.[1,2] Only recently was the partially coherent hopping mechanism introduced as an intermediate between the two conventional ones.[3−5] To distinguish the three CT mechanisms, consider the following: an incoherent transfer in which electrons migrate only between nearest-neighbor states and a superexchange transfer in which electrons take a direct route from donor to acceptor bypassing bridge states, i.e., virtual bridges. Initially tag an electron and follow its movement over time. Within the incoherent hopping mechanism, electrons can only take incoherent transfers throughout the process. On the other hand, within the coherent superexchange mechanism, electrons can only take superexchange transfers. It is also possible that electrons take incoherent and superexchange transfers alternatively over time, hence, the partially coherent hopping mechanism.

For a donor−bridge−acceptor triad, the aforementioned three mechanisms account for all the possible pathways. However, for long-range CT systems, for instance, a system with four states, i.e., donor−bridge−bridge−acceptor, there exist in fact additional pathways that may participate in transferring charges between states: while Figure 1a represents pathways that have been considered conventionally, next-nearest-neighbor hopping pathways, i.e., coherent through-bridge pathways, shown in Figure 1b are also possible, yet have been ignored. Therefore, it is important to examine the role of other coherent through-bridge pathways for comprehensive understanding of CT processes. As for the superexchange transfers, hopping between distant states arises from the coherence within a system.

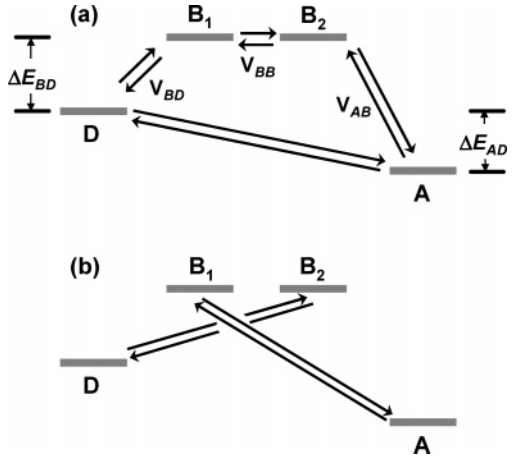

Figure 1. Charge transfer pathways for a system with two consecutive bridges: (a) conventionally considered incoherent nearest-neighbor hopping and coherent superexchange pathways and (b) coherent through-bridge pathways. Energy gaps, ΔE, and coupling constants, V, for simulations performed in this letter are listed in Table 1.

Nevertheless, coherent through-bridge pathways in Figure 1b differ from the superexchange pathways where bridges function solely as a virtual bridge. Therefore, hereafter, we refer to the CT processes that are dominated by pathways through any bridge state in the system as a *through-bridge* mechanism. In particular, for a system with two consecutive bridge states, the through-bridge mechanism consists of the incoherent nearest-neighbor hopping pathways in Figure 1a with the next-nearest-neighbor hopping pathways shown in Figure 1b. At first glance, the coherent hopping between the donor (D) and its distant bridge (B_2) or the acceptor (A) and its distant bridge (B_1) may not seem feasible. In Figure 1b, however, while D and A are separated by two bridges, D (A) and B_2 (B_1) are separated only by a single bridge state. After one considers exponential decrease

* Corresponding author. Email-address: esim@yonsei.ac.kr. Fax: +82-2-364-7050.

10.1021/jp062941p CCC: $33.50

of the effective coupling constant through space with respect to the distance, it is obvious that the magnitude of the effective coupling between D (A) and B_2 (B_1) should always be large compared to that of D and A superexchange interaction. As the bridge array is extended, the probability of coherent pathways between even more distant states may also become significant depending on the coherence within a system.

For coherent systems, short-range CT processes are often governed by the coherent superexchange mechanism. On the other hand, the incoherent nearest-neighbor hopping mechanism has been considered to dominate long-range CT processes.[6−10] Nevertheless, determination of the CT mechanism has been based on the distance dependence of rate constants: the rate constants of the incoherent hopping mechanism are less sensitive to the distance change, while those of the coherent superexchange mechanism decrease exponentially.[6,9,10] Therefore, quantitative analysis on the relative contribution of coherent through-bridge pathways will provide crucial insight into understanding the long-range CT mechanism. We have shown that the on-the-fly filtered propagator functional path integral (OFPF-PI) method provides numerically accurate real-time dynamics of systems embedded in a dissipative medium.[11] Furthermore, the OFPF-PI method is highly useful for the purpose of this letter, since the OFPF-PI method combined with the density matrix decomposition allows evaluation of the contribution of each CT pathway independently and iteratively.[12]

The letter is organized as follows: In section 2, we discuss the OFPF-PI formalism along with the pathway separation in which the reduced density matrix of the system coupled to a dissipative environment is obtained iteratively. Section 3 is devoted to analysis of the quantum mechanical CT pathways and their quantitative contribution. Two series of configurations with different degrees of coherence are considered. For each series, we evaluate the CT dynamics of the system with up to three bridge states. Concluding remarks appear in section 4.

2. Through-Bridge Charge Transfer Mechanism

Details of the OFPF-PI approach can be found elsewhere.[4,11−14] Thus, in this letter, we only briefly discuss the methodology. Consider a one-dimensional CT system, represented by a tight-binding model

$$\mathbf{H}_s = \begin{pmatrix} 0 & V_{BD} & 0 & \cdots & 0 \\ V_{BD} & \Delta E_{BD} & V_{BB} & & \vdots \\ 0 & V_{BB} & \ddots & V_{BB} & 0 \\ \vdots & & V_{BB} & \Delta E_{BD} & V_{AB} \\ 0 & \cdots & 0 & V_{AB} & \Delta E_{AD} \end{pmatrix} \quad (1)$$

This interacts with a thermal bath, which consists of a large number of harmonic oscillators. The direct coupling constants between distant states are set to zero in order to examine the role of effective superexchange interaction owing to the coherence within the configuration. Environments such as the thermal bath are described by the ohmic form of the spectral density, which is characterized by the reorganization energy, λ_{AB}, between the acceptor and its nearest-neighbor bridge and also by the bath cutoff frequency, ω_c. Potential parameters used in this letter are summarized in Table 1, and a typical configuration of a donor−bridge−bridge−acceptor is schematically drawn in Figure 1.

A useful quantity for extracting characteristics of CT dynamics is the reduced density matrix, which is defined as

$$\tilde{\boldsymbol{\rho}}(t) = \mathrm{Tr}_b[\mathrm{e}^{-iHt/\hbar}\boldsymbol{\rho}(0)\,\mathrm{e}^{iHt/\hbar}] \quad (2)$$

TABLE 1: Potential Parameters for the Charge Transfer Systems[a]

	ΔE_{BD}	ΔE_{AD}	V_{BD}	V_{BB}	V_{AB}	λ_{AB}	ω_c
N	500	−400	22	50	135	900	600
M	3790	−775	202	202	202	796	1700

[a] Units are cm^{-1}.

Diagonal elements of $\tilde{\boldsymbol{\rho}}(t)$ provide the time evolution of the charge population in the corresponding state. In eq 2, Tr_b denotes the trace with respect to all bath degrees of freedom, and $\boldsymbol{\rho}(0)$ is the initial density matrix of the whole system including the environment. Assuming that the bath is initially at thermal equilibrium and the system−bath interaction is switched on at $t = 0$, Feynman and Vernon's influence functional path integral discretization gives rise to[15,16]

$$\tilde{\boldsymbol{\rho}}(t) = \sum_{\substack{i \\ \text{all paths}}} \mathbf{S}(\Gamma_i^{(N)})\mathbf{I}(\Gamma_i^{(N)}) \quad (3)$$

where the summation runs for all possible pathways connecting donor and acceptor and $\Gamma_i^{(N)}$ represents the ith pathway that spans time 0 to $t = N\Delta t$. In eq 3, **S** represents the system propagator that includes the initial system density matrix and one-dimensional forward and backward bare system short-time propagators, while **I** is the influence functional that arises from the Gaussian integration of the bath degrees of freedom.[11]

To attain computational efficiency in path integration of eq 3, which suffers from the memory effect owing to the nonlocal influence functional, the OFPF-PI method rewrites eq 3 as a product of history and memory terms;[11]

$$\tilde{\boldsymbol{\rho}}(t) = \sum_i \mathscr{T}(\Gamma_i^{(N-1)})\mathscr{P}^{\mathbf{e}}(\Gamma_i^{(N)}) \quad (4)$$

The history term $\mathscr{T}$ only depends on the past time points from 0 to $t - \Delta t$; in contrast, the memory term $\mathscr{P}^{\mathbf{e}}$ includes interactions between present and past time points. By separating history and memory terms and by utilizing the finite-time bath memory of the dissipative medium, iterative evaluation of the reduced density matrix becomes possible, and the vast number of redundant calculations is omitted. Furthermore, on-the-fly filtering of paths with insignificant weight, i.e., the paths with the integrand in eq 4 smaller than a predetermined cutoff weight, is performed such that the number of paths to be integrated increases subexponentially.[13] Since the OFPF-PI mimics exact integration in a filtered trajectory space without employing any statistical sampling, contributing CT pathways are guaranteed to be taken into account depending on the predetermined cutoff weight. If the cutoff weight is lowered to a very small value, simulated results by the OFPF-PI systematically converges to that of the exact integration.

Since each CT pathway is independent in eq 4, it is also possible to selectively sum the weight of pathways with desired characteristics, for instance, pathways that only take nearest-neighbor hopping, next-nearest-neighbor hopping, or superexchange transfers. Therefore, for long-range CT systems, one can decompose the density matrix as the following[4,12,14]

$$\tilde{\boldsymbol{\rho}}(t) = \tilde{\boldsymbol{\rho}}^b(t) + \tilde{\boldsymbol{\rho}}^c(t) + \tilde{\boldsymbol{\rho}}^p(t) + \tilde{\boldsymbol{\rho}}^s(t) \quad (5)$$

where $\tilde{\boldsymbol{\rho}}^b(t)$ corresponds to through-bridge, $\tilde{\boldsymbol{\rho}}^c(t)$ to coherent superexchange, $\tilde{\boldsymbol{\rho}}^p(t)$ to the partially coherent hopping, and $\tilde{\boldsymbol{\rho}}^s(t)$ to static mechanism. Although the static mechanism does not contribute to the transfer, inclusion of the static pathway is important for the path generation. In particular, for a system

with two consecutive bridges, the partial density matrix of the through-bridge mechanism consists of the nearest-neighbor hopping and the next-nearest-neighbor hopping ($\tilde{\rho}^{n-n}(t)$) contributions such that $\tilde{\rho}^b(t) = \tilde{\rho}^n(t) + \tilde{\rho}^{n-n}(t)$. Partial density matrix of each mechanism can then be evaluated through a pathway sorting. By sorting pathways to the corresponding mechanism, partial contributions of each mechanism are summed as the relative contribution and the role of the individual mechanism are determined. The pathway sorting provides quantitative insights for a specific mechanism without additional rate constant dependencies on length and temperature.

3. Results and Discussion

In this section, we analyze the contribution of the bridge-mediated pathways by varying the number of bridge states and the coherence within the CT system (N and M series in Table 1). For each series in Table 1, CT dynamics in three configurations are evaluated: Nn and Mn configurations with $n = 1$, 2, and 3, where n represents the number of bridge states in the system; thus, the dimension of the system Hamiltonian matrix in eq 1 becomes $(n + 2) \times (n + 2)$. Potential parameters for the N1 and M1 configurations have been adapted from a mutant of purple bacterial photosynthetic reaction center[12] and a short DNA sequence of 5′-GAGGG-3′, respectively.[14] For the long-range CT, we assume all bridge states are equivalent in energy and the coupling between neighboring bridge states is equal to V_{BB}. According to previous studies, the N1 configuration is known to be dominated by the incoherent nearest-neighbor hopping mechanism such that charges transfer to the acceptor through a single bridge. On the other hand, the M1 configuration is known to be dominated by the interplay between incoherent and coherent migrations. In other words, the CT dynamics of the M1 configuration is moderately coherent, while that of the N1 configuration stays incoherent.

In Figure 2, diagonal elements of the reduced density matrices for N1, N2, and N3 configurations are presented. Decay of the donor population ($\tilde{\rho}_{11}$) and rise of the acceptor ($\tilde{\rho}_{33}$ in Figure 2a, $\tilde{\rho}_{44}$ in Figure 2b, and $\tilde{\rho}_{55}$ in Figure 2c) populations are observed. By comparing time evolutions of the reduced density matrix obtained by integrating contributions of all possible pathways ($\tilde{\boldsymbol{\rho}}$), nearest-neighbor hopping pathways only ($\tilde{\boldsymbol{\rho}}^n$), and through-bridge pathways only ($\tilde{\boldsymbol{\rho}}^b(t) = \tilde{\boldsymbol{\rho}}^n(t) + \tilde{\boldsymbol{\rho}}^{n-n}(t)$), it is clearly seen that the converged results are obtained as long as the contribution of the nearest-neighbor hopping pathways are included. It indicates that the dynamics of N1, N2, and N3 all are dominated by the nearest-neighbor hopping pathways such that they are governed by the conventional incoherent hopping mechanism.

For the M1 configuration, however, the dynamics is quite different from that of the N1 configuration, as displayed by the discrepancy between $\tilde{\boldsymbol{\rho}}$ and $\tilde{\boldsymbol{\rho}}^n$ in Figure 3a. With the increased number of bridges, it was expected that the CT mechanism shifts toward the incoherent regime. In Figure 3b,c, however, the agreement between $\tilde{\boldsymbol{\rho}}$ and $\tilde{\boldsymbol{\rho}}^n$ becomes even poorer compared with Figure 3a. This is somewhat unexpected on the basis of the general understanding of the relationship between the donor−acceptor distance and the CT mechanism. More interestingly, by integrating contributions of the through-bridge pathways, $\tilde{\boldsymbol{\rho}}$ and $\tilde{\boldsymbol{\rho}}^b$ are in excellent agreement in Figure 3b and c. This indicates that, in addition to the nearest-neighbor hopping pathways, there are additional coherent through-bridge pathways which contribute substantially for M2 and M3 configurations and they should not be neglected in discussing long-range CT mechanisms. Owing to the convergence, it was found that the

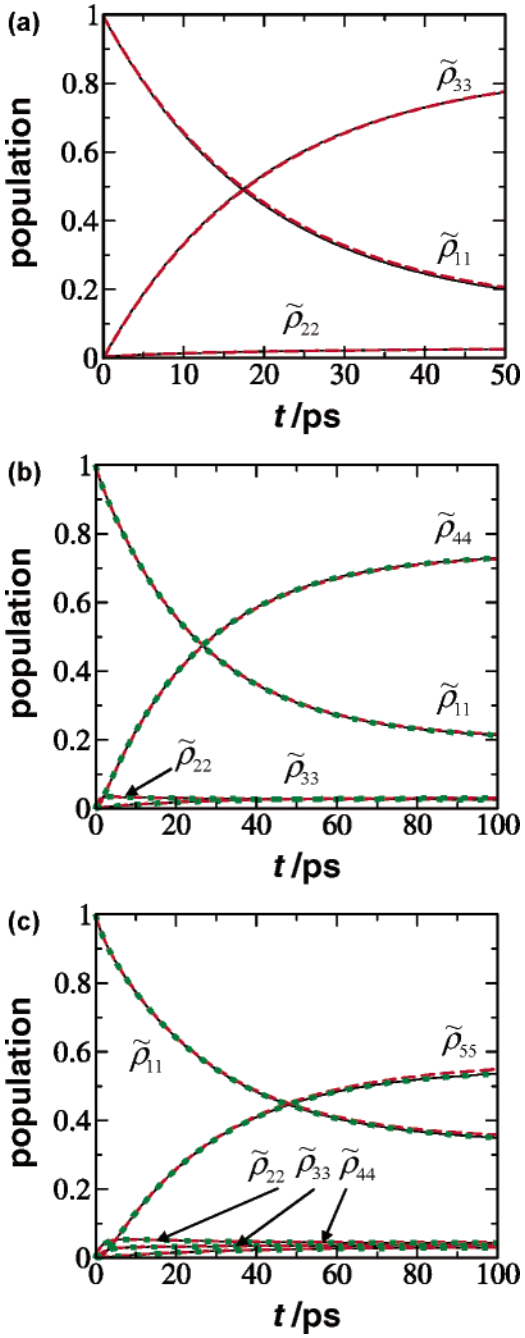

Figure 2. Diagonal elements of the reduced density matrix for the N series given in Table 1 with (a) a single bridge, (b) two bridges, and (c) three bridges. Decay of the donor population ($\tilde{\rho}_{11}$) and rise of the acceptor ((a) $\tilde{\rho}_{33}$, (b) $\tilde{\rho}_{44}$, and (c) $\tilde{\rho}_{55}$) populations. Path integrations of the contributions of all possible pathways ($\tilde{\boldsymbol{\rho}}$, black solid lines), incoherent nearest-neighbor hopping pathways only ($\tilde{\boldsymbol{\rho}}^n$, red dashed lines), and through-bridge pathways only ($\tilde{\boldsymbol{\rho}}^b$, green solid markers) are presented.

governing mechanism for both M2 and M3 configurations is through-bridge CT mechanism.

In fact, coherent transfers other than superexchange have been discussed in various experimental and theoretical works. In particular, considering the CT in DNA sequences, Giese and co-workers speculated that charges coherently migrate from a G/C base pair to a nearest G/C base pair through virtually involved A/T base pairs in between. The overall long-range CT is led by consecutive short-range coherent transfers between closely located relatively stable G/C oxidative states; called G-hopping CT mechanism.[17,18] On the other hand, it has been

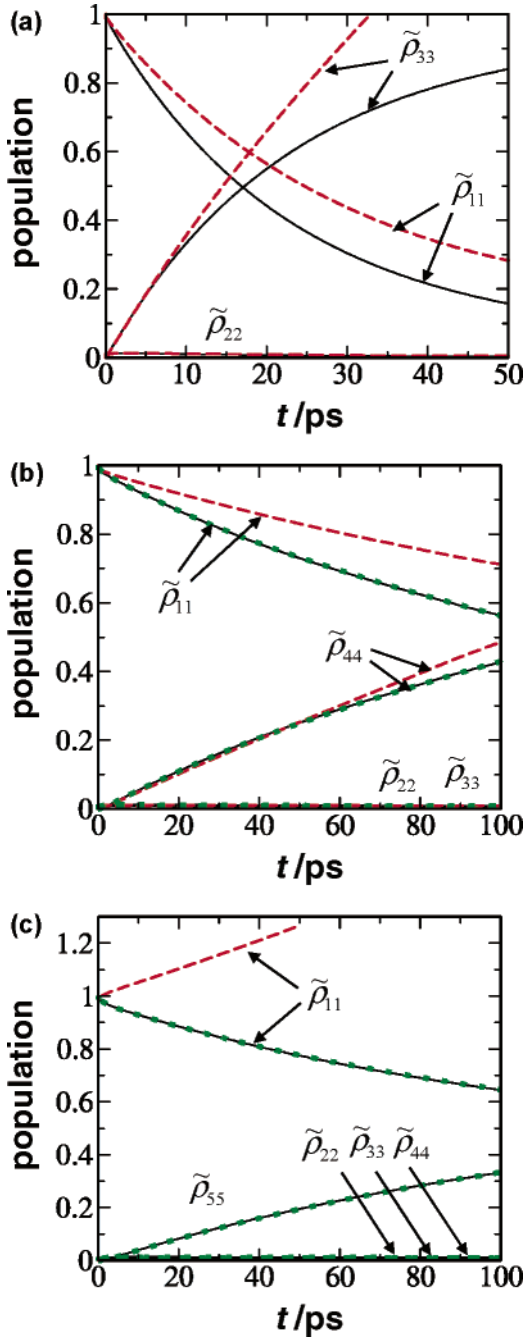

Figure 3. Same as Figure 2 for the M series given in Table 1.

postulated that a "self-trapped" local distortion of the DNA occurs, and the overall transport was governed by the polaronic transition owing to the large electronic overlap between bases.[5,19] The driving force of both the G-hopping and the polaronic transition is the coherence within the system: although the whole system is not perfectly coherent, a subset of the system may remain coherent.

Potential parameters of the energy gaps and the electronic couplings of the M series in Table 1 have been used to model DNA sequences elsewhere.[20,21] Nonetheless, it is currently difficult to argue that the M*n* configuration models the CT process of 5′-G(A)$_n$GGG-3′ DNA sequences, since the spectral densities used in the M*n* configurations were chosen arbitrarily such that the reorganization energy, λ_{AB}, and the bath cutoff frequency, ω_c, are maintained constant. While it is well-known that the reorganization energy varies with the DNA sequence, dependence of the reorganization energy with respect to the

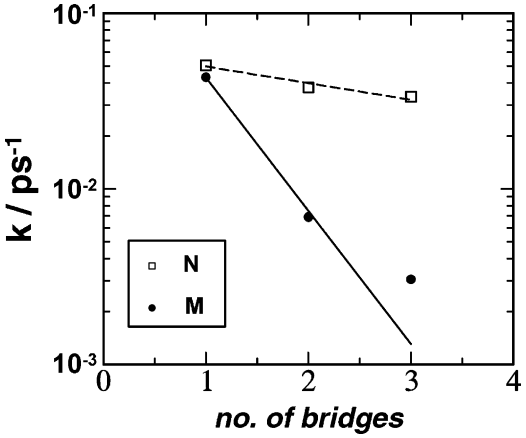

Figure 4. Dependence of charge transfer rate constants on the number of bridges. Open squares correspond to the N series and solid circles to the M series. Dashed and solid lines are exponential fits of the rate constant for the N and M series, respectively.

sequence is relatively unknown.[22,23] Therefore, the findings for the M series cannot be generalized to discuss the CT mechanism of DNA sequences unless a realistic description of the environmental effect is modeled.

Rate constant dependence on the number of bridges has also been investigated. We have assumed a single exponential for the rise of the acceptor population and determined the transfer rate constant. Figure 4 exhibits the difference in the distance dependence of the two series of configurations. For the N series, as anticipated for the incoherent nearest-neighbor hopping mechanism, the rate constant is rather insensitive to the change of the bridge length. On the other hand, the transfer rate constants markedly decrease with the distance for the M series. It has been discussed that the rate constant of the coherent superexchange mechanism decreases exponentially as $k \propto \exp(-\beta R_{DA})$. Exponential fits of the simulated rate constant dependence on donor−acceptor distance are also presented in Figure 4 with the exponents $\beta = 0.064$ Å^{-1} and 0.514 Å^{-1} for the N and M series, respectively. Although the rate constant of the M3 configuration slightly deviates from the fit, the value of the exponent for the M series lies within the range of typical values for CT systems with highly conjugated organic bridges, 0.2−0.6 Å^{-1}. [24]

In summary, the N series is governed by the incoherent nearest-neighbor hopping mechanism regardless of the number of bridges, in contrast to the M series, governing mechanism of which shifts from the interplay between the incoherent nearest-neighbor hopping and the partially coherent hopping mechanism for short-ranges to the through-bridge mechanism for long-ranges.

4. Concluding Remarks

In this letter, we have explored the contribution of through-bridge pathways in the long-range CT processes. Numerically accurate time evolution of the charge population has been obtained using the path integral approach by sorting CT pathways according to their characteristics. Conventionally, the incoherent hopping has been almost exclusively considered equivalent to the nearest-neighbor hopping. Thus, coherent migrations between states other than superexchange donor−acceptor transfer have been neglected, particularly for cases with high-energy bridges. While recently investigated experimental and theoretical studies have actively discussed that the governing CT mechanism undergoes a change from the coherent superexchange to the incoherent hopping mechanism as a function

of the donor−acceptor distance, the results presented therein lack quantitative description of the relative contribution of the individual mechanism. To the knowledge of the authors, systematic and quantitative investigation on the coherent through-bridge pathways, such as next-nearest-neighbor hopping pathways, within the molecular wire-type CT processes, was presented for the first time. For the coherent system considered in this letter, the long-range CT mechanism was determined to be governed not by the conventional incoherent hopping mechanism, but rather by the through-bridge mechanism. The findings are highly useful for understanding the long-range CT processes and are expected to contribute significantly to unraveling the relationship between system configuration and CT mechanism.

Acknowledgment. This work was supported by the Korea Research Foundation Grant funded by the Korean Government (MOEHRD) (KRF 2005-204-C00027). The authors also acknowledge the Molecular Science Research Institute at Yonsei University.

References and Notes

(1) May, V.; Kuhn, O. *Charge and Energy Transfer Dynamics in Molecular Systems*, 2nd ed.; Wiley-VCH: New York, 2004.
(2) Wagenknecht, H.-A. *Charge Transfer in DNA: From Mechanism to Application*; Wiley-VCH: New York, 2005.
(3) Zhang, H.; Li, X.-Q.; Hang, P.; Yu, X. Y.; Yan, Y. *J. Chem. Phys.* **2002**, *117*, 4578.
(4) Sim, E. *J. Phys. Chem. B* **2005**, *109*, 11829.
(5) Henderson, P. T.; Jones, D.; Hampikian, G.; Kan, Y.; Schuster, G. B. *Proc. Natl. Acad. Sci. U.S.A.* **1999**, *96*, 8353.
(6) Giese, B.; Amaudrut, J.; Kohler, A. K.; Spormann, M.; Wessely, S. *Nature (London)* **2001**, *412*, 318.
(7) Davis, W. B.; Svec, W. A.; Ratner, M. A.; Wasielewski, M. R. *Nature (London)* **1998**, *396*, 60.
(8) Long, Y.-T.; Abu-Irhayem, E.; Kraatz, H.-B. *Chem.—Eur. J.* **2005**, *11*, 5186.
(9) Bixon, M.; Jortner, J. *Chem. Phys.* **2002**, *281*, 393.
(10) Petrov, E. G.; Shevchenko, Y. V.; May, V. *Chem. Phys.* **2003**, *288*, 269.
(11) Sim, E. *J. Chem. Phys.* **2001**, *115*, 4450.
(12) Sim, E. *J. Phys. Chem. B* **2004**, *108*, 19093.
(13) Sim, E.; Kim, H. *J. Phys. Chem. B* In press.
(14) Kim, H.; Sim, E. *J. Phys. Chem. B* **2006**, *110*, 631.
(15) Feynman, R. P.; Hibbs, A. R. *Quantum Mechanics and Path Integrals*; McGraw-Hill: New York, 1965.
(16) Feynman, R. P.; Vernon, J. F. L. *Ann. Phys.* **1963**, *24*, 118.
(17) Meggers, E.; Michel-Beyerle, M. E.; Giese, B. *J. Am. Chem. Soc.* **1998**, *120*, 12950.
(18) Giese, B.; Wessely, S.; Spormann, M.; Lindemann, U.; Meggers, E.; Michel-Beyerle, M. E. *Angew. Chem., Int. Ed.* **1999**, *38*, 996.
(19) Chang, J.; Miller, W. H. *J. Chem. Phys.* **1987**, *87*, 1648.
(20) Voityuk, A. A.; Jortner, J.; Bixon, M.; Rösch, N. *Chem. Phys. Lett.* **2000**, *324*, 430.
(21) Voityuk, A. A.; Jortner, J.; Bixon, M.; Rösch, N. *J. Chem. Phys.* **2001**, *114*, 5614.
(22) Siriwong, K.; Voityuk, A. A.; Newton, M. D.; Rösch, N. *J. Phys. Chem. B* **2003**, *107*, 2595.
(23) Lebard, D. N.; Lilichenko, M.; Matyushov, D. V.; Berlin, Y. A.; Ratner, M. A. *J. Phys. Chem. B* **2003**, *107*, 14509.
(24) Segal, D.; Nitzan, A.; Davis, W. B.; Wasielewski, M. R.; Ratner, M. A. *J. Phys. Chem. B* **2000**, *104*, 3817.